

Microscopic Calculation of Six-Body Inelastic Reactions with Complete Final State Interaction: Photoabsorption of ${}^6\text{He}$ and ${}^6\text{Li}$

Sonia Bacca,¹ Mario Andrea Marchisio,¹ Nir Barnea,² Winfried Leidemann,¹ and Giuseppina Orlandini¹

¹*Dipartimento di Fisica, Università di Trento and INFN (GC Trento), I-38050 Povo, Trento, Italy*

²*The Racah Institute of Physics, The Hebrew University, 91904, Jerusalem, Israel*

(Received 20 December 2001; published 15 July 2002)

Six-body inelastic reactions are calculated microscopically including the full six-nucleon final state interaction. The total cross sections of $\gamma + {}^6\text{He} ({}^6\text{Li}) \rightarrow X$ are considered as examples. The Lorentz integral transform method and the effective interaction approach for the hyperspherical formalism are employed. While ${}^6\text{Li}$ has a single broad giant resonance peak, there are two well separated peaks for ${}^6\text{He}$ corresponding to the breakup of the neutron halo and the α core, respectively. The comparison with the few available experimental data is discussed.

DOI: 10.1103/PhysRevLett.89.052502

PACS numbers: 21.45.+v, 24.30.Cz, 25.20.Dc, 31.15.Ja

Inelastic responses of A -body systems are fundamental physical quantities, since they contain valuable information about the dynamical structure of the system. Microscopic calculations of such responses are particularly important to reveal fine details of the dynamics and of the reaction mechanism. However, calculations of final state wave functions (FSWF) for energies with various open channels are already rather complicated for a three-body system and presently out of reach for $A > 3$. On the other hand, it has been shown that the extremely complicated microscopic calculation of the FSWF is not necessary, since the response can be calculated with the Lorentz integral transform (LIT) method [1], where only a bound-state-like problem has to be solved. As pointed out in [1] the method can be applied in few- and many-body systems. Though the FSWF is not calculated, final state interaction (FSI) effects on the response are taken rigorously into account. There are quite a few examples for the application of this approach to few-body nuclei up to $A = 4$ (see, e.g., Refs. [2–5]). As to bound-state calculations there has been tremendous progress for systems with $A > 4$ in the last decade. This is due not only to an increase of the numerical power of modern computers but also to various new microscopical approaches [6–9]. Traditionally systems with a number of particles between 4 and about 15 are considered neither few- nor many-body systems and thus establish a transition region where few- and many-body physics have to merge eventually. In the present work we present a microscopic calculation of an inelastic reaction of a six-body system, thus taking a step towards an accurate microscopic explanation for typical many-body aspects, e.g., collective phenomena.

We apply the LIT method and solve the above mentioned bound-state-like problem via an expansion in hyperspherical harmonics (HH) within the recently developed effective interaction HH (EIHH) approach [9]. The response of a system to real photons is a fundamental quantity; therefore, we have chosen the total photoabsorption cross sections of the six-body nuclei as an inelastic

response to study. It is important to note that photoabsorption experiments with such light nuclei were performed some 20–30 years ago and that the activity has not been carried on further, in part because of missing theoretical guidance. In the last few years there has been renewed interest, however, mainly for halo nuclei (see, e.g., [10]).

Since this is the first microscopic calculation of a six-body inclusive reaction with consideration of the complete FSI, we take central nucleon-nucleon (NN) potential models, namely, the semirealistic potentials Malfliet-Tjon, version I-III (MTI-III) [11], and Minnesota (MN) [12], with parameters as given in [9]. The MTI-III model contains Yukawa-type potentials and has a strong short range repulsion, while the MN model consists of Gauss-type potentials and has a rather soft core. The MTI-III potential is fitted to the NN scattering S -wave phase shifts, 1S_0 and 3S_1 , up to about pion threshold, whereas the MN potential is fitted to low-energy two- and three-body data. Calculations of the total photoabsorption cross sections of three- and four-body nuclei have already been performed with the LIT method with such semirealistic potentials [3,4,13], and recently, for ${}^3\text{H}$ and ${}^3\text{He}$, also with realistic NN and three-nucleon forces [5]. The calculations for three-body nuclei show that semirealistic potentials lead to a rather realistic description of the total photoabsorption cross section. Though for six-body systems the missing P -wave interaction could play some role, we believe that the main features of the calculated cross sections are close to the results of a more realistic calculation.

The total photoabsorption cross section is given by

$$\sigma(\omega) = 4\pi^2\alpha\omega R(\omega), \quad (1)$$

where α is the fine structure constant and

$$R(\omega) = \int d\Psi_f |\langle \Psi_f | \hat{O} | \Psi_0 \rangle|^2 \delta(E_f - E_0 - \omega) \quad (2)$$

is the response function; $|\Psi_{0/f}\rangle$ and $E_{0/f}$ denote wave

function and energy of ground and final state, respectively, while \hat{O} is the transition operator. For the photoabsorption cross section the Siegert theorem leads to

$$\hat{O} = \hat{D}_z = \sum_{i=1}^A \frac{\tau_i^3 z_i'}{2}. \quad (3)$$

Here τ_i^3 and z_i' represent the third component of the isospin operator and of the coordinate of the i th particle in the center of mass frame, respectively. It is well known that the dipole approximation is excellent for the total photoabsorption cross section (see, e.g., [14]).

In the LIT method one obtains $R(\omega)$ from the inversion of the transform

$$L(\sigma_R, \sigma_I) = \int d\omega \frac{R(\omega)}{(\omega - \sigma_R)^2 + \sigma_I^2} = \langle \tilde{\Psi} | \tilde{\Psi} \rangle, \quad (4)$$

where the Lorentz state $\tilde{\Psi}$ is found as a unique solution of the ‘‘Schrödinger-like’’ equation

$$(H - E_0 - \sigma_R + i\sigma_I) |\tilde{\Psi}\rangle = \hat{D}_z |\Psi_0\rangle. \quad (5)$$

Since the right-hand side of Eq. (5) is localized and since there is an imaginary part σ_I , one has an asymptotic boundary condition similar to a bound state. Therefore one can apply bound-state techniques for its solution. We expand Ψ_0 and $\tilde{\Psi}$ in terms of the six-body symmetrized HH [15]. The expansion is performed up to maximal values K_{\max}^0 and K_{\max} of the HH grand-angular quantum number K for Ψ_0 and $\tilde{\Psi}$, respectively. In the case of Ψ_0 the basis states are constructed with the quantum numbers of the ground state. With a central S -wave interaction for ${}^6\text{He}$ (${}^6\text{Li}$) one has angular momentum $L = 0$ (0), spin $S = 0$ (1), isospin $T = 1$ (0) with a third component $T_z = -1$ (0). For $\tilde{\Psi}$ the basis functions possess the quantum numbers selected by the dipole transition: $L = 1$ (1), $S = 0$ (1), $T = 1$ and 2 (1), and $T_z = -1$ (0). We improve the convergence of the HH expansion using the recently de-

veloped EIH approach [9] where the bare potential is replaced by an effective potential constructed via the Suzuki-Lee method [16]. In convergence, however, the same results as with the bare potential are obtained (see Ref. [9]).

In order to evaluate the LIT we calculate the quantity $\langle \tilde{\Psi} | \tilde{\Psi} \rangle$ directly using the Lanczos algorithm [17] instead of solving the Schrödinger-like equation (5). In fact, starting from the first Lanczos vector

$$|\varphi_0\rangle = \frac{\hat{D}_z |\Psi_0\rangle}{\sqrt{\langle \Psi_0 | \hat{D}_z^\dagger \hat{D}_z | \Psi_0 \rangle}} \quad (6)$$

and applying recursively the following relations,

$$b_{n+1} |\varphi_{n+1}\rangle = H |\varphi_n\rangle + a_n |\varphi_n\rangle - b_n |\varphi_{n-1}\rangle, \quad (7)$$

$$a_n = \langle \varphi_n | H | \varphi_n \rangle, \quad b_n = \|\langle b_n | \varphi_n \rangle\|, \quad (8)$$

where a_n and b_n are the Lanczos coefficients, one finds that the LIT can be written as a continuous fraction

$$L(\sigma_R, \sigma_I) = \frac{1}{\sigma_I} \text{Im} \frac{\langle \Psi_0 | \hat{D}_z^\dagger \hat{D}_z | \Psi_0 \rangle}{(z - a_0) - \frac{b_1^2}{(z - a_1) - [b_2^2 / (z - a_2) - b_3^2 \dots]}}. \quad (9)$$

As shown in [17] a rapid convergence is reached.

For ${}^6\text{Li}$ the numerator of Eq. (9) can be evaluated directly as the ground state expectation value of long range operators (mean square charge radius $\langle r_{\text{ch}}^2 \rangle$, mean square proton-proton distance $\langle r_{\text{pp}}^2 \rangle$),

$$\langle \Psi_0 | \hat{D}_z^\dagger \hat{D}_z | \Psi_0 \rangle = \frac{1}{3} \left[Z^2 \langle r_{\text{ch}}^2 \rangle - \frac{Z(Z-1)}{2} \langle r_{\text{pp}}^2 \rangle \right], \quad (10)$$

that converges rapidly in the EIH approach. For ${}^6\text{He}$ the situation is different, because there are two final isospin channels ($T = 1, 2$). Therefore one has to sum over both channels, replacing Eq. (9) by

$$L(\sigma_R, \sigma_I) = \frac{1}{\sigma_I} \langle \Psi_0 | \hat{D}_z^\dagger \hat{D}_z | \Psi_0 \rangle \times \text{Im} \sum_T \frac{\alpha_{K_{\max}}^T}{[z - a_0(T)] - \frac{b_1^2(T)}{[z - a_1(T)] - [b_2^2(T) / [z - a_2(T)] - b_3^2(T) \dots]}}}, \quad (11)$$

where $a_n(T)$ and $b_n(T)$ are the Lanczos coefficients for the corresponding T channels, and

$$\alpha_{K_{\max}}^T = \frac{\sum_{\text{HH}^T}^{K_{\max}} \langle \Psi_0 | \hat{D}_z^\dagger | \text{HH}^T \rangle \langle \text{HH}^T | \hat{D}_z | \Psi_0 \rangle}{\sum_T \sum_{\text{HH}^T}^{K_{\max}} \langle \Psi_0 | \hat{D}_z^\dagger | \text{HH}^T \rangle \langle \text{HH}^T | \hat{D}_z | \Psi_0 \rangle}. \quad (12)$$

The sum $\sum_{\text{HH}^T}^{K_{\max}}$ runs over all the HH basis functions with isospin T and $K \leq K_{\max}$.

Now we turn to the discussion of the results. First, in Table I we present various ground state properties. From the estimated errors one sees that a rather good convergence is obtained. Note that the DD values can be calculated in two ways: as a ground state expectation value and

by an integration of $R(\omega)$. Corresponding results differ very little showing a good internal consistency of our calculation. In Fig. 1 we show the photoabsorption cross section $\sigma(\omega)$ of ${}^6\text{Li}$ with the MTI-III and of ${}^6\text{He}$ with the MN potential for various K_{\max} . One observes a rather satisfactory convergence. For both nuclei one notes that the peak heights decrease slightly with increasing K_{\max} . While the low-energy $\sigma(\omega)$ is rather stable for ${}^6\text{Li}$, strength is shifted towards lower ω for ${}^6\text{He}$. From the convergence behavior we estimate errors of less than 10%, and we expect that mostly peak heights and much less the general shape of $\sigma(\omega)$ will be affected by possibly missing contributions from higher K .

TABLE I. Binding energy (E_B), root mean square matter radius (r_m), and ground state expectation value in Eq. (10) (DD) for ${}^6\text{He}$ and ${}^6\text{Li}$ with MN and MTI-III potentials (Coulomb force included). The numbers in parentheses are an estimate of the error due to the convergence behavior.

| Nucleus | V_{NN} | K_{\max}^0 | E_B (MeV) | r_m (fm) | DD (fm) |
|-----------------|----------|--------------|-------------|------------|-----------|
| ${}^6\text{He}$ | MN | 10 | -30.48(10) | 2.37(4) | 2.28(15) |
| | MTI-III | 10 | -31.87(10) | 2.23(4) | 1.99(10) |
| ${}^6\text{Li}$ | MN | 12 | -34.90(10) | 2.18(2) | 1.50(2) |
| | MTI-III | 12 | -35.88(20) | 2.13(2) | 1.51(1) |

In Fig. 2 we show our final results for both NN potentials. Though the MTI-III model leads to somewhat higher cross section peaks, one obtains rather similar pictures of $\sigma(\omega)$ with both potentials. Note that there is one single giant dipole resonance peak for ${}^6\text{Li}$ and two well separated peaks for ${}^6\text{He}$. The low-energy ${}^6\text{He}$ peak of the $T = 1$ channel at $\omega = 7.5$ MeV (MN) and 9.5 MeV (MTI-III) is due to the breakup of the neutron halo. The second one, at about $\omega = 35$ MeV, corresponds to the breakup of the α core and has contributions from both T channels (about 40% of strength due to the $T = 2$ channel). The ${}^6\text{Li}$ cross section does not show such a substructure. This is probably due to the fact that the breakup into two three-body nuclei, ${}^3\text{He} + {}^3\text{H}$, fills the gap between the halo and the α core peaks. Note that in the case of ${}^6\text{He}$ a corresponding breakup into two identical nuclei, ${}^3\text{H} + {}^3\text{H}$, is not induced by the dipole operator. We have also integrated the various cross sections up to 100 MeV and find the following enhancements κ_{TRK} of the Thomas-Reiche-

Kuhn (TRK) sum rule [59.74 NZ/A MeV mb(1 + κ_{TRK}): 0.42 (${}^6\text{Li}$, MN), 0.47 (${}^6\text{Li}$, MTI-III), 0.45 (${}^6\text{He}$, MN), and 0.50 (${}^6\text{He}$, MTI-III).

We already mentioned that we do not expect that the semirealistic central S -wave potentials lead to realistic results in all details. In particular, an additional P -wave interaction should affect somewhat the low-energy cross section. Nevertheless, we think it is instructive to compare with experiment. In Fig. 3(a) the results of a recent ${}^6\text{He}$ experiment [10,18] are shown. The cross section was extracted from the ${}^6\text{He}$ Coulomb excitation using a secondary radioactive ${}^6\text{He}$ beam. Close to threshold the theoretical cross section has a different shape than the experimental one. We should mention that a better threshold behavior is obtained in a cluster model description of ${}^6\text{He}$ with an inert α core and two neutrons interacting with it via a P -wave potential [22,23]. Additional information comes from a recent ${}^6\text{Li}({}^7\text{Li}, {}^7\text{Be}){}^6\text{He}$ experiment [24] where an E1 resonance of ${}^6\text{He}$ is found at $\omega = 8.5$ MeV (width 15 MeV). This result is not too different from our low-energy peak. A similar value for the excitation energy is found in a no-core-shell-model calculation with realistic NN interactions [25].

In the case of ${}^6\text{Li}$ the experimental situation is more complex (note that there is no transition of the isovector dipole operator to the $T = 0$ $d + \alpha$ channel). The semi-inclusive channel ${}^6\text{Li}(\gamma, \sum_n)$ measured in Ref. [19] corresponds to the total $\sigma(\omega)$ only at $\omega \leq 15.7$ MeV. At higher ω , channels not involving neutrons open up (${}^3\text{He} + {}^3\text{H}$, ${}^3\text{H} + p + d$). Regarding these two channels we show experimental data from Refs. [20,21]. To make the

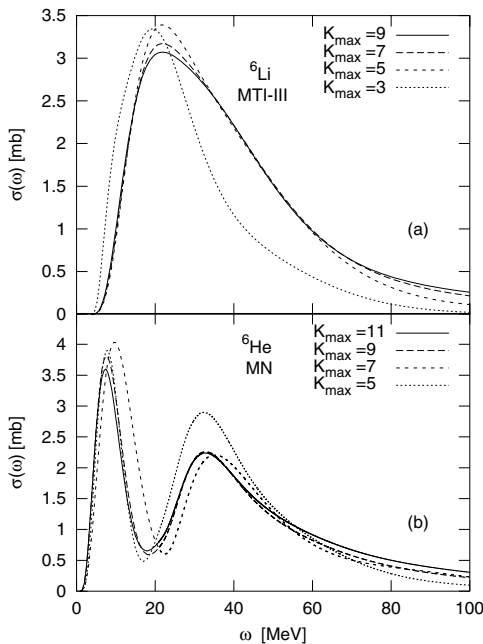


FIG. 1. Cross section $\sigma(\omega)$ with various values of K_{\max} : ${}^6\text{Li}$ with MTI-III (a) and ${}^6\text{He}$ with MN potentials (b).

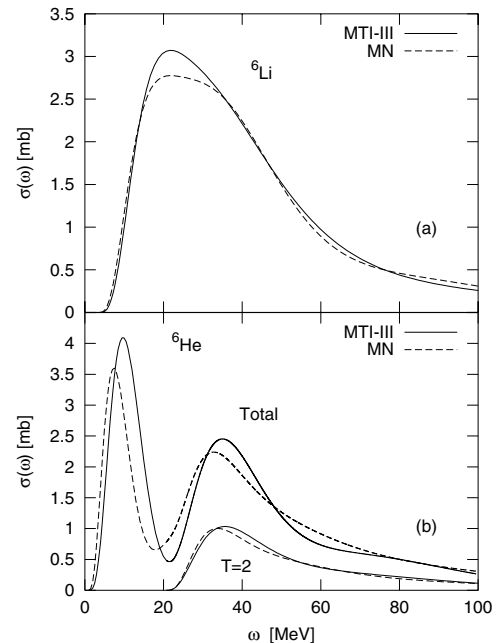


FIG. 2. Cross section $\sigma(\omega)$ with both NN potentials: ${}^6\text{Li}$ (a), ${}^6\text{He}$ with channel $T = 2$ and sum of $T = 1$ and 2 (total) (b).

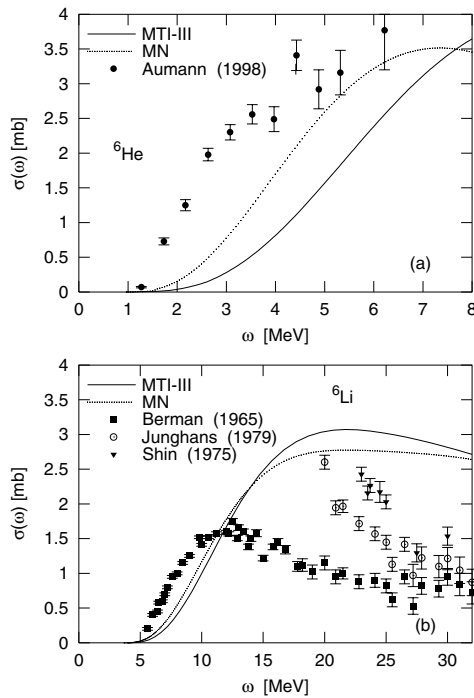


FIG. 3. Theoretical and experimental results for cross section $\sigma(\omega)$: ${}^6\text{He}$ (theoretical curves are convoluted with the Gaussian instrumental response function [10,18]) (a), ${}^6\text{Li}$ with experimental data from [19–21] (see text) (b).

comparison simpler we have summed these data with those of [19] [see Fig. 3(b)]. At low ω there is a similar difference of theoretical and experimental results as for the ${}^6\text{He}$ case. The comparison does not improve with increasing ω . On the other hand, the experimental situation is not settled as one can note from the different results of Refs. [20,21].

In the following we summarize our results briefly. We present the first microscopic calculation of an inelastic six-body cross section considering the complete six-body FSI. To this end we make use of the LIT method [1] and expand ground and Lorentz states in hyperspherical harmonics via the EIH approach [9]. The LIT is calculated with the help of the Lanczos technique [17]. The calculated total photoabsorption cross sections of ${}^6\text{He}$ and ${}^6\text{Li}$ show rather different structures. While ${}^6\text{Li}$ exhibits a single broad giant resonance peak, one clearly distinguishes two well separated peaks for ${}^6\text{He}$. The low-energy peak is due to the breakup of the ${}^6\text{He}$ neutron halo, whereas the second peak corresponds to the breakup of the α core. A comparison with experimental data shows that the theoretical cross sections have a different shape at threshold, which is presumably explained by the missing P -wave interaction in the employed semirealistic central S -wave potentials. The situation in the giant dipole peak region is much less clear, either because of the lack of experimental data (${}^6\text{He}$) or because existing data do not lead to a unique picture (${}^6\text{Li}$). It is evident that further experimental activities are necessary in order to shed more light on the six-nucleon photoabsorption cross sections. On the other hand, further

progress has also to be made in theory, in particular, by addressing the question of the role of P -wave interactions in the total photoabsorption cross section of the six-body nuclei.

We thank T. Aumann and P. Grabmayr for helpful discussions concerning the experimental data. This work was supported by the Italian Ministry of Research.

-
- [1] V.D. Efros, W. Leidemann, and G. Orlandini, Phys. Lett. B **338**, 130 (1994).
 - [2] V.D. Efros, W. Leidemann, and G. Orlandini, Phys. Rev. Lett. **78**, 432 (1997).
 - [3] V.D. Efros, W. Leidemann, and G. Orlandini, Phys. Rev. Lett. **78**, 4015 (1997).
 - [4] N. Barnea, V.D. Efros, W. Leidemann, and G. Orlandini, Phys. Rev. C **63**, 057002 (2001).
 - [5] V.D. Efros, W. Leidemann, G. Orlandini, and E.L. Tomusiak, Phys. Lett. B **484**, 223 (2000); Nucl. Phys. A **689**, 421c (2001).
 - [6] R.B. Wiringa, Steven C. Pieper, J. Carlson, and V.R. Pandharipande, Phys. Rev. C **62**, 014001 (2000).
 - [7] Y. Suzuki and K. Varga, *Stochastic Variational Approach to Quantum Mechanical Few-Body Systems* (Springer-Verlag, Berlin, 1998).
 - [8] P. Navrátil and B.R. Barrett, Phys. Rev. C **59**, 1906 (1999); P. Navrátil, J. Vary, and B.R. Barrett, Phys. Rev. C **62**, 054311 (2000).
 - [9] N. Barnea, W. Leidemann, and G. Orlandini, Phys. Rev. C **61**, 054001 (2000); Nucl. Phys. A **693**, 565 (2001).
 - [10] T. Aumann *et al.*, Phys. Rev. C **59**, 1252 (1999).
 - [11] R.A. Malfliet and J.A. Tjon, Nucl. Phys. A **127**, 161 (1969).
 - [12] D.R. Thomson, M. LeMere, and Y.C. Tang, Nucl. Phys. A **286**, 53 (1977); I. Reichstein and Y.C. Tang, *ibid.* A **158**, 529 (1970).
 - [13] V.D. Efros, W. Leidemann, and G. Orlandini, Phys. Lett. B **408**, 1 (1997).
 - [14] H. Arenhövel and M. Sanzone, Few-Body Syst. Suppl. **3**, 1 (1991).
 - [15] N. Barnea and A. Novoselsky, Ann. Phys. (N.Y.) **256**, 192 (1997); and Phys. Rev. A **57**, 48 (1998).
 - [16] K. Suzuki and S.Y. Lee, Prog. Theor. Phys. **64**, 2091 (1980).
 - [17] M.A. Marchisio, N. Barnea, W. Leidemann, and G. Orlandini, e-print nucl-th/0202009.
 - [18] T. Aumann (private communication).
 - [19] B.L. Berman, R.L. Bramblett, J.T. Caldwell, R.R. Harvey, and S.C. Fultz, Phys. Rev. Lett. **15**, 727 (1965).
 - [20] G. Junghans, K. Bangert, U.E.P. Berg, R. Stock, and K. Wienhard, Z. Phys. A **291**, 353 (1979).
 - [21] Y.M. Shin, D.M. Skopik, and J.J. Murphy, Phys. Lett. **55B**, 297 (1975).
 - [22] A. Cobis, D.V. Fedorov, and A.S. Jensen, Phys. Rev. Lett. **79**, 2411 (1997).
 - [23] B.V. Danilin, I.J. Thompson, J.S. Vaagen, and M.V. Zhukov, Nucl. Phys. A **632**, 383 (1998).
 - [24] S. Nakayama *et al.*, Phys. Rev. Lett. **85**, 262 (2000).
 - [25] P. Navrátil, J.P. Vary, W.E. Ormand, and B.R. Barrett, Phys. Rev. Lett. **87**, 172502 (2001).